

# Supporting Information

Brockhoff et al. 10.1073/pnas.0913862107

## SI Materials and Methods

**In Vitro Mutagenesis of hTAS2Rs.** Site-directed mutagenesis of hTAS2R cDNAs was done by PCR-mediated recombination. Briefly, a two-step PCR protocol was applied to generate two subfragments. The 5' subfragments were amplified with the vector-specific CMV forward primer and the reverse mutagenesis primer, the corresponding 3' subfragments were obtained using the complementary forward mutagenesis primer together with the vector-specific BGH reverse primer. PCR conditions were: 5 min, 95 °C; 15 cycles: 1 min annealing [annealing temperatures were calculated using the formula:  $T \approx T_{\text{melt}} - 3 \text{ } ^\circ\text{C} - (3 \text{ } ^\circ\text{C} \times \text{mismatching bp})$ ], 0.5 to 2.5 min 72 °C, 30 s 95 °C, followed by 5 min annealing, 10 min 72 °C. For the subsequent PCR-reaction, both purified subfragments were mixed and amplified using CMV forward primer and BGH reverse primer. PCR conditions were: 5 min, 95 °C, 15 cycles: 2 min, 54 °C, 3 min, 72 °C, 30 s, 95 °C, followed by 5 min, 54 °C, 10 min 72 °C. For the generation of chimeric receptors, we used forward primers containing sequences complementary to the cDNA of the parental TAS2R designated to become the 5'-part of the chimera on one end and a sequence complementary to the cDNA of the parental TAS2R designated to become the 3'-part of the

chimera on the other end. Finally, the constructs were cloned and sequenced. For subcloning either the vector pcDNA5/FRT-sst3-MCS-hsv or pcDNA5/FRT-sst3-MCS-GFP<sup>2</sup> were used resulting in the addition of an N-terminal sst3-tag and a C-terminal hsv-tag or GFP<sup>2</sup>-tag, respectively. For a list of oligonucleotides, see Table S3.

**Functional Expression.** For functional expression analyses the receptor cDNAs were transfected into HEK 293T cells stably expressing the G protein chimera G $\alpha$ 16gust44, incubated for 22 h, loaded with the calcium sensitive dye Fluo-4 AM, and washed with C1 solution (130 mM NaCl, 5 mM KCl, 10 mM Hepes, 2 mM CaCl<sub>2</sub>, 10 mM glucose, pH 7.4). Test substances were diluted in C1 solution. Changes in cytosolic calcium levels were recorded in a fluorometric imaging plate reader (Molecular Devices). Data were collected from at least two independent experiments carried out in duplicates. Fluorescence signals were corrected for responses of mock-transfected cells and normalized to background fluorescence. Dose-response relations and EC<sub>50</sub> values were calculated in SigmaPlot (SPSS) by nonlinear regression using the function  $f(y) = \{(a - d)/[1 + (x/EC_{50})^{nH}] + d\}$ .

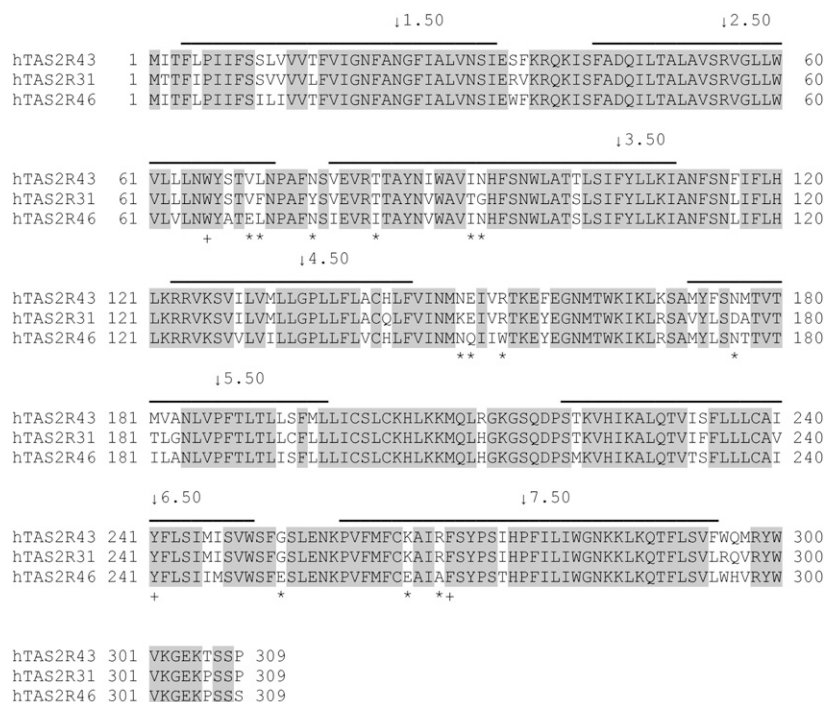


**Fig. S1.** Alignment of the amino acid sequences of the receptors hTAS2R43, -R31, and -R46. Identical positions are highlighted in gray. The transmembrane regions are indicated by solid lines and the reference positions according to Ballesteros-Weinstein numbering are labeled. The Ballesteros-Weinstein numbering was introduced for Rhodopsin-like GPCRs, whereas the T2R family belongs to the Taste/Freezled family (1). Nevertheless, we could identify the bitter taste family positions analogous to each transmembrane (TM) domain's most conserved position identified in the Ballesteros-Weinstein numbering. These positions (1.50 in TM1, 2.50 in TM2, etc.) are shown by arrows. Positions different between hTAS2R46 and hTAS2R43 or hTAS2R31 that were mutated are labeled by asterisks, positions mutated to support the position of strychnine docking in the hTAS2R46 model are labeled by (+).

1. Lagerström MC, Schiöth HB (2008) Structural diversity of G protein-coupled receptors and significance for drug discovery. *Nat Rev Drug Discov* 7:339–357.

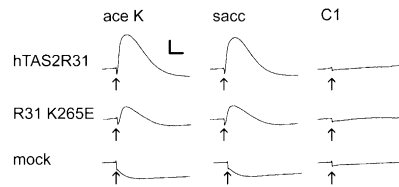
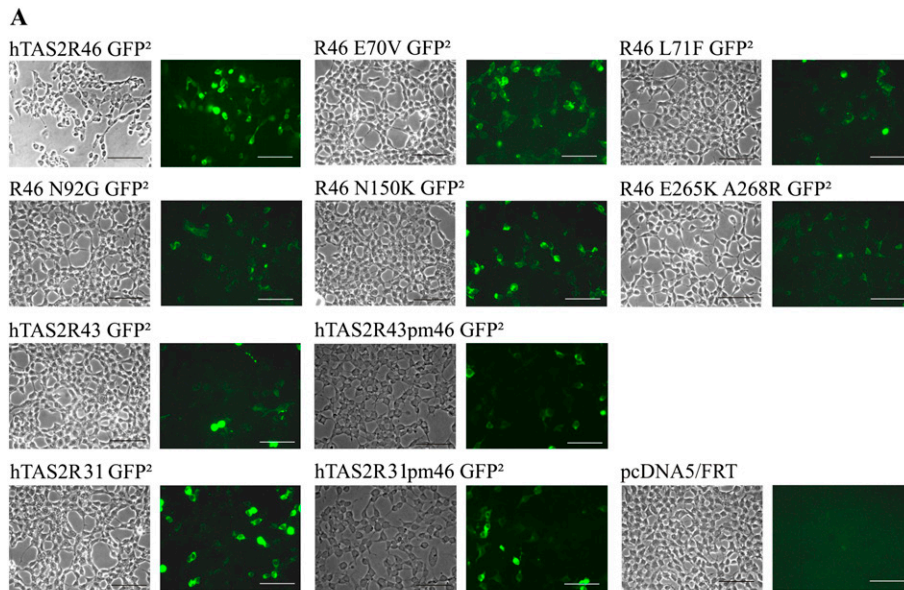


**Fig. S2.** Calcium transients of cells transfected with hTAS2R31, mutant hTAS2R31 K265E (R31 K265E) and empty vector (mock) upon bath application (arrows) of acesulfame K (ace K, 10 mM), saccharin (sacc, 10 mM), and C1 buffer (C1). Transients were averaged from triplicates. y axis, 2,000 counts; x axis, 1 min.

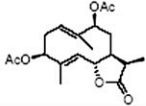
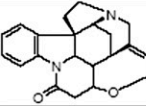
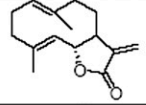
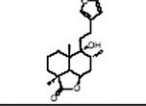
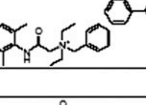
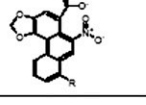


**B**

Construct	Expression in %
hTAS2R46 GFP	19 ± 6
hTAS2R46 E70V GFP	23 ± 7
hTAS2R46 L71F GFP	8 ± 1
hTAS2R46 N92G GFP	15 ± 2
hTAS2R46 N150K GFP	15 ± 2
hTAS2R46 E265K A268R GFP	16 ± 4
hTAS2R43 GFP	11 ± 1
hTAS2R43pm46 GFP	17 ± 2
hTAS2R31 GFP	19 ± 3
hTAS2R31pm46 GFP	19 ± 4

**Fig. S3.** Expression of hTAS2R-constructs in HEK293 cells. (A) Brightfield and fluorescence images of GFP-fusion proteins of selected hTAS2R46 constructs used in functional calcium imaging experiments. A fraction of HEK293 cells express the transfected constructs as indicated by their green fluorescence. (Scale bars, 200  $\mu$ M.) (B) Quantification of the expression rates obtained for GFP-fusion constructs. The number of green fluorescent cells was counted and expressed as percentage of all cells visible under brightfield illumination. Note that the expression rates of constructs that exhibited reduced responses in functional calcium imaging for all tested agonists (hTAS2R46 L71F, -N92G, -N150K), and thus may be suspected to suffer from deficits in their general expression rates, show expression rates comparable to the hTAS2R46 wild-type receptor. However, a minor contribution for the observed reduced functional responsiveness of mutant receptor hTAS2R46 L71F may arise from reduced heterologous expression.

**A**

hTAS2R46 agonist	structure	threshold ( $\mu\text{M}$ )	Number of putative interaction sites					
			H-acc.	H-donor	Neg.	pos.	hydrophobic	rings
Sintenin		0.03	6	0	0	0	3	0
Strychnine		0.1	2	0	0	1	5	1
Costunolide		0.3	2	0	0	0	3	0
Marrubiin		0.3	4	1	4	0	0	1
Denatonium		30	1	1	0	1	2	2
Aristol. Acid*		0.1	2	0	1	0	0	3

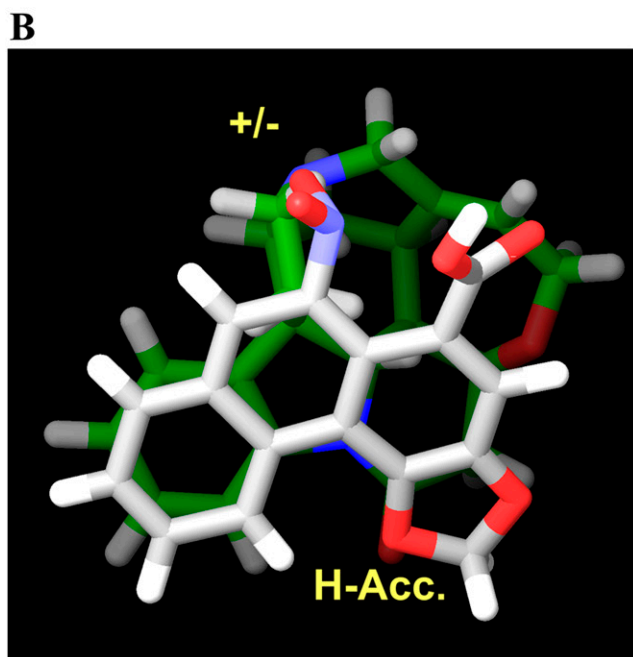


**Fig. S4.** Comparison of chemical and structural features of hTAS2R46 agonists. (A) Shown are five agonists that activate heterologously expressed hTAS2R46 with different threshold concentrations and aristolochic acid, which is not an agonist for hTAS2R46 wild-type but activates the hTAS2R46 mutant, hTAS2R46 E265K A268R, starting from a threshold concentration of 0.1  $\mu\text{M}$ . The number of putative interaction sites as determined using the software "Phase" is compiled according to the chemical nature of the sites as putative hydrogen-acceptors (H-acc.), hydrogen-donors (H-donor), negatively charged group (neg.), positively charged group (pos.), hydrophobic groups (hydrophobic), and aromatic ring systems (rings). Agonists differ vastly from each other both in terms of numbers of putative interaction sites as well as with respect to their mode of putative interaction. Comparison of the putative interaction sites reveal several features important for docking considerations: (i) All agonists contain at least one putative hydrogen bond acceptor site and, if hydrophobic interaction sites and aromatic ring systems are grouped together, at least two hydrophobic sites are available for receptor interaction. Therefore, theoretically a common pharmacophore may consist of one hydrogen acceptor site and two hydrophobic sites or ring systems. (ii) The most potent activators, excluding the substance marrubiin, exhibit no hydrogen bond donor site, which makes an important hydrogen acceptor site within the receptor unlikely. Thus, the compared agonists indicate rather multiple contact sites between receptor and the various agonists rather than the stable anchoring of substances at more than one or two receptor residues. Only two hTAS2R46 agonists contain a positively charged putative interaction site. Interestingly, a loss of activation of hTAS2R46<sub>E265K A268R</sub>

Legend continued on following page

by these two agonists is observed, whereas the negatively charged aristolochic acid now activates the mutated receptor. The complementary mutation in hTAS2R43 and -R31 also causes a switch between the charged agonists. These observations strongly suggest that strychnine binding to hTAS2R46 involves an ionic interaction with residues located in the upper part of TM7, perhaps supplemented by the formation of hydrogen bonds and hydrophobic interactions. (B) Overlay of the chemical structures of aristolochic acid and strychnine. Overlaying of the structures of strychnine (background, green carbon atoms) and aristolochic acid (foreground, gray carbon atoms) demonstrate that both molecules with respect to the chemical groups considered to play a major role in their activation of bitter taste receptors, namely the putative hydrogen bond acceptor site (H-Acc.) and the opposing charges ( $^{+/-}$ ), congruently fit on top of each other. This feature may explain why exchanging charged amino acid residues by oppositely charged residues in bitter taste receptors hTAS2R46 and hTAS2R31 lead to a switch in agonist selectivities.

↓ 7.50

```

bOPSD      FMTIPAFFAKTSAVYNPVIYIMMNKQFRNCMVTTI
hTAS2R46   VFMFCEAIAFSYEPSTHFFILWGNKKLKQTFLSVL
OR1E1      DTVMAMYTTVVTEPMLNPFYISLRNRDMKGALSSRVI
  
```

**Fig. S5.** Alignment of TM7 of bovine rhodopsin (bOPSD), hTAS2R46, and mouse olfactory receptor OR1E1. The reference position (7.50, arrow) according to Balesteros-Weinstein numbering is labeled. Identical positions are highlighted in gray. The positions in hTAS2R46 identified in this study to be involved in agonist binding (E265<sup>7,39</sup> and A268<sup>7,42</sup>) and predicted to be involved in agonist interaction of odorant receptors by Man et al. (1) (corresponding to alignment positions 322 and 325 compared with table 1 and figure 2 of ref. 1) are printed in bold and underscored.

1. Man O, Gilad Y, Lancet D (2004) Prediction of the odorant binding site of olfactory receptor proteins by human-mouse comparisons. *Protein Sci* 13:240–254.

**Table S1. Extended agonist spectra of hTAS2R46 and point-mutated receptors hTAS2R31pm46 and hTAS2R43pm46**

Substance	EC <sub>50</sub> in $\mu$ M		
	hTAS2R46	hTAS2R31pm46	hTAS2R43pm46
Absinthin	9.9 $\pm$ 0.3	2.2 $\pm$ 0.6	4.8 $\pm$ 1.4
Andrographolide	19.7 $\pm$ 0.7	11.4 $\pm$ 2.1	19.1 $\pm$ 1.9
Denatonium	54.2 $\pm$ 6.2	18.2 $\pm$ 9.9	32.9 $\pm$ 7.5
Marrubiin	18.3 $\pm$ 3.6	7.8 $\pm$ 0.6	25.2 $\pm$ 3.1
Parthenolide	15.0 $\pm$ 0.8	17.4 $\pm$ 0.3	22.2 $\pm$ 3.7
Picrotoxinin	138.8 $\pm$ 9.3	160.8 $\pm$ 2.4	150.5 $\pm$ 4.9
Santamarin	8.5 $\pm$ 2.2	3.3 $\pm$ 2.0	9.9 $\pm$ 1.5
Sintenin	0.56 $\pm$ 0.08	0.10 $\pm$ 0.03	0.48 $\pm$ 0.11
Strychnine	0.43 $\pm$ 0.02	0.31 $\pm$ 0.05	0.45 $\pm$ 0.10

Functionally relevant hTAS2R46 residues identified in this study were collected in recipient receptors hTAS2R31 and -R43, resulting in the constructs hTAS2R31pm46 (hTAS2R31 V70E F71L T82I G92N K150N D176N G253E K265E R268A) and hTAS2R43pm46 (hTAS2R43 V70E T82I G253E K265E R268A), respectively. All nine substances used for this experiment, except santamarin and denatonium, activate only hTAS2R46 wild-type, but not hTAS2R43 or hTAS2R31. The hTAS2R43 wild-type receptor responds already to high concentrations of denatonium (threshold  $\sim$ 300  $\mu$ M, Fig. 1B and ref. 1) and santamarin (threshold  $\sim$ 100  $\mu$ M). Therefore, the observed activation of the mutant hTAS2R43pm46 by santamarin and denatonium indicates an increased sensitivity caused by the transfer of hTAS2R46-specific residues but not a gain-of-responsiveness, whereas all other activations of hTAS2R31pm46 and hTAS2R43pm46 by hTAS2R46-specific agonists reflect a transfer in agonist-specificity.

1. Behrens M, et al. (2009) The human bitter taste receptor hTAS2R50 is activated by the two natural bitter terpenoids andrographolide and amarogentin. *J Agric Food Chem* 57: 9860–9866.

**Table S2. Point mutagenesis of hTAS2R46 residues located in proximity to strychnine docked into the receptor in silico model**

Construct	Strychnine [ $\mu$ M]
hTAS2R46	EC <sub>50</sub> = 0.43 $\pm$ 0.02
hTAS2R46 W66A	Threshold = 3
hTAS2R46 Y241F	EC <sub>50</sub> = 1.00 $\pm$ 0.31
hTAS2R46 F269N	No response

To confirm that molecular modeling of hTAS2R46 and subsequent docking of strychnine into the receptor model resulted in reasonable localization of the agonist, selected residues, which should be located in close proximity to the strychnine molecule and were not part of our template-guided mutagenesis, were analyzed. Note that amino acid exchanges in all tested positions that were predicted to be located near to strychnine in silico also affect receptor responsiveness in functional calcium imaging experiments, thus corroborating the modeling results.

**Table S3. Oligonucleotides used for the construction of receptor chimeras and in vitro mutagenesis**

Construct	Oligonucleotide	Sequence (5' to 3')
Receptor chimeras		
hTA2R46tm3-31 and hTAS2R31tm3-46	R46_R31tm3_for R46_R31tm3_rev	GCTCAAGATTGCCAATTTCTCC GGAGAAATGGCAATCTTGAGC
hTAS2R46il3-31 and hTAS2R31il3-46	R46_R31il3_for R46_R31il3_rev	GTTCTCTGTGTAACATCTC GAGATGTTTACACAGAGAAC
hTAS2R46 mutagenesis		
hTAS2R46 <sub>W66A</sub>	R46 <sub>W66A</sub> _for R46 <sub>W66A</sub> _rev	GTATTAATGCGTATGCAACTGAGTTGAATCC GGATTCAACTCAGTTGCATACGCATTTAATAC
hTAS2R46 <sub>E70V</sub>	R46 <sub>E70V</sub> _for R46 <sub>E70V</sub> _rev	GTATGCAACTGTGTTGAATCCAG CTGGATTCAACACAGTTGCATAC
hTAS2R46 <sub>E70D</sub>	R46 <sub>E70D</sub> _for R46 <sub>E70D</sub> _rev	GTATGCAACTGACTTGAATCCAG CTGGATTCAAGTCAGTTGCATAC
hTAS2R46 <sub>E70Q</sub>	R46 <sub>E70Q</sub> _for R46 <sub>E70Q</sub> _rev	GTATGCAACTCAGTTGAATCCAG CTGGATTCAACTGAGTTGCATAC
hTAS2R46 <sub>E70A</sub>	R46 <sub>E70A</sub> _for R46 <sub>E70A</sub> _rev	GTATGCAACTGCGTTGAATCCAG CTGGATTCAACGCAGTTGCATAC
hTAS2R46 <sub>E70K</sub>	R46 <sub>E70K</sub> _for R46 <sub>E70K</sub> _rev	GTATGCAACTAAGTTGAATCCAG CTGGATTCAACTTAGTTGCATAC
hTAS2R46 <sub>E70S</sub>	R46 <sub>E70S</sub> _for R46 <sub>E70S</sub> _rev	GTATGCAACTTCGTTGAATCCAG CTGGATTCAACGAAGTTGCATAC
hTAS2R46 <sub>L71F</sub>	R46 <sub>L71F</sub> _for R46 <sub>L71F</sub> _rev	GTATGCAACTGAGTTCAATCCAG CTGGATTGAACTCAGTTGCATAC
hTAS2R46 <sub>N76Y</sub>	R46 <sub>N76Y</sub> _for R46 <sub>N76Y</sub> _rev	CCAGCTTTTACAGTATAGAAG CTTCTATACTGTAAAAAGCTGG
hTAS2R46 <sub>I82T</sub>	R46 <sub>I82T</sub> _for R46 <sub>I82T</sub> _rev	GAAGTAAGAACTACTGCTTACAATG CATTGTAAGCAGTAGTTCTTACTTC
hTAS2R46 <sub>I91T</sub>	R46 <sub>I91T</sub> _for R46 <sub>I91T</sub> _rev	GTCTGGGCAGTAACCAACCATTTC GAAATGGTTGTTACTGCCAGAC
hTAS2R46 <sub>N92G</sub>	R46 <sub>N92G</sub> _for R46 <sub>N92G</sub> _rev	CTGGGCAGTAATCGGCCATTTTC GAAATGGCCGATTACTGCCAG
hTAS2R46 <sub>N150K</sub>	R46 <sub>N150K</sub> _for R46 <sub>N150K</sub> _rev	GTGATAAACATGAAGCAGATTATATGGAC GTCCATATAATCTGCTTCAATGTTTATCAC
hTAS2R46 <sub>Q151E</sub>	R46 <sub>Q151E</sub> _for R46 <sub>Q151E</sub> _rev	GTGATAAACATGAATGAGATTATATGGACAAAAG CTTTTGTCCATATAATCTCATTTCATGTTTATCAC
hTAS2R46 <sub>W154R</sub>	R46 <sub>W154R</sub> _for R46 <sub>W154R</sub> _rev	CAGATTATACGGACAAAAGAATATG CATATTCTTTTGTCCGTATAAATCTG
hTAS2R46 <sub>N176D</sub>	R46 <sub>N176D</sub> _for R46 <sub>N176D</sub> _rev	GCAATGTACCTTTTTCAGATACAACGGTAAAC GTTACCGTTGTATCTGAAAGGTACATTGC
hTAS2R46 <sub>Y241F</sub>	R46 <sub>Y241F</sub> _for R46 <sub>Y241F</sub> _rev	GTTATGTGCCATTTTCTTTCTGTCCATAATC GATTATGGACGAAAAGAAAATGGCACATAAC
hTAS2R46 <sub>E253G</sub>	R46 <sub>E253G</sub> _for R46 <sub>E253G</sub> _rev	GGAGTTTTGGGAGTCTGGAAAAC GTTTTCCAGACTCCAAAACCTCC
hTAS2R46 <sub>E265K</sub> and hTAS2R46 <sub>E265K</sub> A268R	R46 <sub>E265K</sub> _for R46 <sub>E265K</sub> _rev	CTTCATGTTCTGCAAAGCTATT AATAGCTTTGCAGAACATGAAG
hTAS2R46 <sub>A268R</sub> and hTAS2R46 <sub>E265K</sub> A268R	R46 <sub>A268R</sub> _for R46 <sub>A268R</sub> _rev	GCTATTCGATTCAGCTATCCTTC GAAGGATAGCTGAATCGAATAGC

**Table S3. Cont.**

Construct	Oligonucleotide	Sequence (5' to 3')
hTAS2R46 <sub>E265D</sub>	R46 <sub>E265D</sub> _for	CATGTTCTGCGACGCTATTGC
	R46 <sub>E265D</sub> _rev	GCAATAGCGTCGCAGAACATG
hTAS2R46 <sub>E265Q</sub>	R46 <sub>E265Q</sub> _for	CATGTTCTGCCAAGCTATTGC
	R46 <sub>E265Q</sub> _rev	GCAATAGCTTGGCAGAACATG
hTAS2R46 <sub>F269N</sub>	R46 <sub>F269N</sub> _for	GCTATTGCAAACAGCTATCCTTCAACCC
	R46 <sub>F269N</sub> _rev	GGGTTGAAGGATAGCTGTTTGAATAGC
hTAS2R31 mutagenesis		
hTAS2R31 <sub>K265E</sub>	R31 <sub>K265E</sub> _for	CATGTTCTGCGAAGCTATT
	R31 <sub>K265E</sub> _rev	AATAGCTTCGCAGAACATG
hTAS2R31 <sub>R268A</sub>	R31 <sub>R268A</sub> _for	GCTATTGCATTCAGCTATCCTTC
	R31 <sub>R268A</sub> _rev	GAAGGATAGCTGAATGCAATAGC
hTAS2R31 <sub>K265E R268A</sub> and hTAS2R31pm46	R31 <sub>K265E R268A</sub> _for	CATGTTCTGCGAAGCTATTGCATTCAGC
	R31 <sub>K265E R268A</sub> _rev	GCTGAATGCAATAGCTTCGCAGAACATG
hTAS2R31pm46	R31 <sub>V70E</sub> _for	GGTATTCAACTGAGTTAATCCAGC
	R31 <sub>V70E</sub> _rev	GCTGGATTAACACTCAGTTGAATACC
	R31 <sub>F71L</sub> _for	GGTATTCAACTGAGTTGAATCCAGC
	R31 <sub>F71L</sub> _rev	GCTGGATTCACACTCAGTTGAATACC
	R31 <sub>T82L</sub> _for	GTGTAGAAGTAAGAATTACTGCTTATAATGTCTGG
	R31 <sub>T82L</sub> _rev	CCAGACATTATAAGCAGTAATCTTACTTCTACAC
	R31 <sub>K150N</sub> _for	GTGATAAACATGAATGAGATTGTACGGAC
	R31 <sub>K150N</sub> _rev	GTCCGTACAATCTCATTGTTTATCAC
	R31 <sub>D176N</sub> _for	CAGTGTACCTTTCAAATGCGACTGTAAC
	R31 <sub>D176N</sub> _rev	GTTACAGTCGCATTTGAAAGGTACACTG
	R31 <sub>G253E</sub> _for	GGAGTTTTGAGAGTCTGG
	R31 <sub>G253E</sub> _rev	CCAGACTCTCAAACTCC
hTAS2R43 mutagenesis		
hTAS2R43pm46	R43 <sub>V70E</sub> _for	GGTATTCAACTGAATTGAATCCAGC
	R43 <sub>V70E</sub> _rev	GCTGGATTC AATTCAGTTGAATACC
	R43 <sub>T82L</sub> _for	GTGTAGAAGTAAGAATTACTGCTTATAATATCTGG
	R43 <sub>T82L</sub> _rev	CCAGATATTATAAGCAGTAATCTTACTTCTACAC
	R43 <sub>G253E</sub> _for	CAGTTTGGAGTTTTGAGAGTCTGGAAAAC
	R43 <sub>G253E</sub> _rev	GTTTTCCAGACTCTCAAACTCCAAACTG
	R43 <sub>K265E R268A</sub> _for	GTTCTGCGAAGCTATTGCATTCAGC
	R43 <sub>K265E R268A</sub> _rev	GCTGAATGCAATAGCTTCGCAGAAC
Additional oligonucleotides		
Vector primer	CMV	CTTGTCATCGTCATCCTTGTAGTCAGTTACAGTGCTG
	BGH	GACTACAAGGATGACGATGACAAGTATCAGTTCCAGGC